



HAL
open science

Stray light correction on array spectroradiometers for optical radiation risk assessment in the workplace

A Barlier-Salsi

► **To cite this version:**

A Barlier-Salsi. Stray light correction on array spectroradiometers for optical radiation risk assessment in the workplace. *Journal of the Society for Radiological Protection*, 2014, *J. Radiol.Prot.*, 34 (4), pp.doi:10.1088/0952-4746/34/4/915. 10.1088/0952-4746/34/4/915 . hal-01148941

HAL Id: hal-01148941

<https://hal.science/hal-01148941>

Submitted on 5 May 2015

HAL is a multi-disciplinary open access archive for the deposit and dissemination of scientific research documents, whether they are published or not. The documents may come from teaching and research institutions in France or abroad, or from public or private research centers.

L'archive ouverte pluridisciplinaire **HAL**, est destinée au dépôt et à la diffusion de documents scientifiques de niveau recherche, publiés ou non, émanant des établissements d'enseignement et de recherche français ou étrangers, des laboratoires publics ou privés.

Stray light correction on array spectroradiometers for optical radiation risk assessment in the workplace

A Barlier-Salsi

Institut national de recherche et de sécurité (INRS)

E-mail: annick.barlier-salsi@inrs.fr

Abstract. The European directive 2006/25/EC requires the employer to assess and if necessary measure the levels of exposure to optical radiation in the workplace. Array spectroradiometers can measure optical radiation from various types of sources; however poor stray light rejection affects their accuracy. A stray light correction matrix, using a tunable laser, was developed at the National Institute of Standards and Technology (NIST). As tunable lasers are very expensive, the purpose of this study was to implement this method using only nine low power lasers; other elements of the correction matrix being completed by interpolation and extrapolation. The correction efficiency was evaluated by comparing CCD spectroradiometers with and without correction and a scanning double monochromator device as reference. Similarly to findings recorded by NIST, these experiments show that it is possible to reduce the spectral stray light by one or two orders of magnitude. In terms of workplace risk assessment, this spectral stray light correction method helps determine exposure levels, with an acceptable degree of uncertainty, for the majority of workplace situations. The level of uncertainty depends upon the model of spectroradiometers used; the best results are obtained with CCD detectors having an enhanced spectral sensitivity in the UV range. Thus corrected spectroradiometers require a validation against a scanning double monochromator spectroradiometer before using them for risk assessment in the workplace.

1. Introduction

Workers may be exposed to optical radiation from specialized [1–3] or general use lamps [4,5] or industrial processes [6,7]. In all these working situations, optical radiation has the potential to be harmful. Some guidelines on limits of exposure to incoherent Ultraviolet [8], Visible and Infrared [9,10] radiation have been published by the International Commission on Non-Ionizing Radiation Protection (ICNIRP). These Exposure Limit Values (ELVs) [10-11] have been used in the European directive 2006/25/EC [11], which requires the employer to assess and, if necessary measure and/or calculate the levels of exposure to optical radiation. ELVs are divided into seven potential health effects on the spectral region from 180 to 3000 nm.

Due to the variety of sources and the wide range of the spectrum, there are no accurate, fast, simple, and affordable methods for measuring risk in the workplace. Radiometers can rapidly measure an entire wavelength region [12]; nevertheless to avoid errors, the radiometer should be calibrated with a standard source similar to the tested source [13,14]. This is unconceivable, as radiometers are intended to measure various types of sources in the workplace. Moreover risk assessment covering the seven spectral regions involves using several filtered detectors and the attempts to produce a filter precisely matching the various hazard weighting functions has met with a limited success. Since these filters are related to the ELVs, modifying in the ELVs means changing the device and, furthermore, old measurements would become unusable. This problem currently occurs with the new ELVs [10] proposed by ICNIRP in the Visible and near-IR wave range.

Spectroradiometric measurements, on the other hand, exclusively characterizing the source are independent of ELVs. Consequently, on the wavelength range from 200 to 1000 nm, CCD array spectroradiometers appear to be the more suitable instrument for this application, being portable, affordable and fast compared to scanning double monochromator devices. Although having many advantages, their accuracy is limited by the presence of spectral stray light originating from inter-reflections on the optical elements of the instrument, higher order diffraction, fluorescence, etc. In the best array spectroradiometer, the level of stray light measured at any pixel, is around 10^{-5} for the measurement of a monochromatic source or 10^{-3} for the measurement of a broadband source [15]. Due to the cumulative effects, the stray light observed with a broadband source such as incandescent lamps may cause significant errors, especially in the UV range where the signal is weak compared to the visible range.

Several stray light rejection methods have been described in scientific literature. Optical methods can be applied to suppress the stray light, blocking the unwanted light by using an optical filter wheel [16,17]. This technology is commonly used in scanning spectroradiometers. Various bandpass filters are available in the UVA, visible or near infrared region. However, a suitable shortpass filter which transmits UV radiation at wavelength shorter than 250 nm and rejecting signal at longer wavelength, to our knowledge, does not exist. Numerical methods to reduce stray light errors have also been proposed [15,18–20]. Yianttila *et al* [18] proposed a scatter light correction algorithm where the slit scattering function is determined by measuring a laser line at 633nm. Applying this method allows to obtain adequate accuracy not only for sunbed UV radiation measurements [18] but also for measurements of phototherapy and photobiology sources [21]. Nevertheless this method has only been experimented for UV measurements. An another numerical approach developed by Zong *et al.* [15] at NIST demonstrates that the stray light errors can be reduced by one or two orders of magnitude. The spectrometer's response, using a tunable laser, is characterized for a set of laser lines that cover the instrument's spectral range to derive a correction matrix. The corrected signal is obtained by a simple matrix multiplication. This method based on a tunable laser is also used by Physikalisch Technische Bundesanstalt (PTB) [22–24] to characterize the spectrometer stray light behaviour within the wavelength range of 200 to 1100 nm. This simple solution, easily implemented in acquisition software, has several advantages, with the exception of the high cost

of the tunable laser. For this reason, the method has been simplified [25] for solar applications or adapted [26] using a double monochromator to produce monochromatic lines.

Following the same approach, a method where only a few laser lines are used, is proposed in this study. The correction matrix is based on monochromatic lines produced by nine low power lasers in the 266-980 nm wavelength range; other elements of the correction matrix are completed by interpolation and extrapolation. The experiment consists of measuring several lamps with two commercial CCD array spectroradiometers and a scanning double monochromator device as reference. The correction efficiency was assessed by comparing CCD spectroradiometers with and without correction and the reference instrument on the basis of relative spectral measurements and quantities E_{eff} , E_{UVA} , E_B [11] required to assess exposure levels.

2. Methods

2.1. Stray light correction matrix

2.1.1. Principle. The stray light correction method by Zong *et al.* [15] is clearly explained in paper Ref. [15] and illustrated in figure 1. A spectrometer with n pixels array detector is fully characterized with the help of two indices i and j referring to output and input signal, respectively; i is the pixel index of the array detector and j relates to the wavelength of the excitation line, expressed as pixel space. The method is based on measuring the spectrometer signal on the full spectral range for different monochromatic lines. Response of each pixel i to the monochromatic excitation at wavelength λ_j is called spectral line-spread function (LSF), denoted $f_{LSF\ i,j}$. LSF has two parts: the narrow peak region around $pixel_{i=j}$, called in-band response IB , representing the instrument's bandpass, and the low signal measured at other pixels arising from spectral stray light.

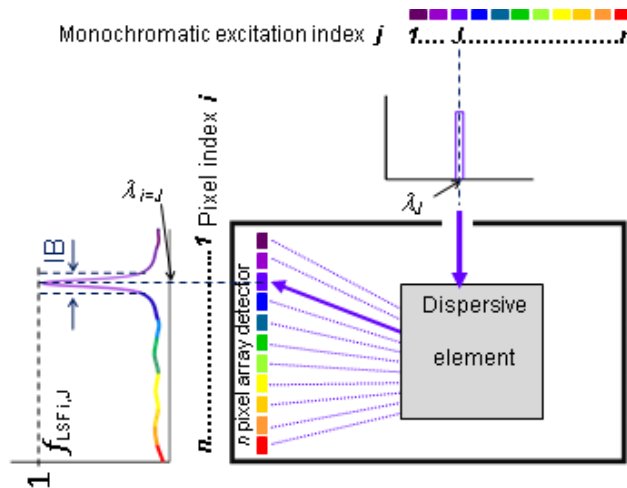


Figure 1. Illustration of the LSF determination with an n pixel array detector.

The stray light distribution function (*SDF*) is obtained by normalizing $f_{LSF\ i,J}$ to the sum of the relative signal in the in-band region *IB* and setting values within the *IB* to zero. The normalized signal $d_{i,J}$, at each pixel *i* due to the monochromatic excitation line *J* is given by:

$$d_{i,J} = \frac{f_{LSF\ i,J}}{\sum_{i \in IB} f_{LSF\ i,J}} \quad \text{for } i \notin IB \quad \text{or} \quad d_{i,J} = 0 \quad \text{for } i \in IB \quad (1)$$

SDF vectors determined at each monochromatic excitation for wavelength λ_j enable the *SDF* matrix *D* ($n \times n$) to be built.

When a broadband source illuminates the *n* pixels of the array detector, the total stray light signal at a given pixel *i*, denoted $y_{sl,i}$ is the sum of stray light contributions from each *IB* signal $y_{IB,j(j=1..n)}$ at wavelength $\lambda_{j(j=1..n)}$ of the broadband source spectra. Thus, the measured signal $y_{meas,i}$ at pixel *i* includes the true *IB* signal $y_{IB,i}$ plus the stray light signal $y_{sl,i}$:

$$y_{meas,i} = y_{IB,i} + y_{sl,i} = y_{IB,i} + \sum_{j=1}^n (d_{i,j} y_{IB,j}) \quad (2)$$

Expressed in terms of matrix, equation 2 gives:

$$Y_{meas} = Y_{IB} + Y_{sl} = Y_{IB} + DY_{IB} = [I + D]Y_{IB} \quad (3)$$

where column vectors Y_{IB} and Y_{meas} represent the in-band signal and the measured signal respectively, and *I* the identity matrix. Then the true spectra Y_{IB} of the broadband source is obtained as follow:

$$Y_{IB} = [I + D]^{-1} Y_{meas} = CY_{meas} \quad (4)$$

where *C* is the stray light correction matrix.

2.1.2. Choosing the *IB* width. Unlike the scanning monochromator device, CCD array spectroradiometers do not have a constant bandwidth across the spectral range. The bandwidth generally increases at higher wavelengths, which means it is not easy to define the width of *IB*. For this reason, the effects of the chosen width of *IB* on the correction matrix and consequently on the corrected signal, were studied for several configurations. On the one hand, *IB* was constant on the full spectral range and defined as $IB=2.4 \times FWHM$ or $IB=3 \times FWHM$; on the other hand, *IB* varied according to the wavelength so that *IB* matches all the values around the peak region for which the signal was higher than 1% of the peak value [27] and defined as $IB=values > 1\%peak$.

2.1.3. Monochromatic sources. Nine low power lasers in the wavelength range 266-980 nm were used as monochromatic sources to create the correction matrix. The monochromatic line at

wavelength $\lambda_j = 266 \pm 1\text{nm}$ required a Q-switched pulsed laser with 3mW of power; other sources were Continuous Wave (CW) lasers with 1mW of power for wavelength $\lambda_j = 405, 447, 473, 532, 589, 633, 808, \text{ and } 980 \pm 5\text{ nm}$.

2.1.4. Process to generate the correction matrix. The initial matrix consists of n rows depending of the number of usable pixels on the detector, and 9 columns. Each column J contains the matching measured spectral line-spread function $f_{LSFmeas\ i,J}$ ($i=1\dots n$); The correction matrix C is obtained from the initial matrix as follow:

- Normalizing $f_{LSFmeas\ i,J}$ by its peak value to obtain $f_{LSFi,J}$,
- Interpolating the columns between the known columns and extrapolating columns outside the known columns to generate an $n \times n$ LSF matrix. Two methods of interpolation/ extrapolation were experimented: cubic spline and linear. Interpolation and extrapolation were performed along the matrix diagonals. Because extrapolation becomes impossible where there is only one point left, which is the case in the both high right and low left quarters of the matrix, the last calculated diagonal was copied to complete the remaining diagonal.
- Normalizing the $n \times n$ LSF matrix according to equation 1 and adding identity matrix. Thus, $[I+D]$ matrix has the following form :

$$[I + D] = \begin{bmatrix} 1 & 0 & 0 & \dots & d_{1,j} & \dots & d_{1,n-2} & d_{1,n-1} & d_{1,n} \\ 0 & 1 & 0 & \dots & d_{2,j} & \dots & d_{2,n-2} & d_{2,n-1} & d_{2,n} \\ 0 & 0 & 1 & \dots & d_{3,j} & \dots & d_{3,n-2} & d_{3,n-1} & d_{3,n} \\ \vdots & \vdots & \vdots & \dots & \vdots & \dots & \vdots & \vdots & \vdots \\ d_{i,1} & d_{i,2} & d_{i,3} & \dots & 1 & \dots & d_{i,n-2} & d_{i,n-1} & d_{i,n} \\ \vdots & \vdots & \vdots & \dots & \vdots & \dots & \vdots & \vdots & \vdots \\ d_{n-2,1} & d_{n-2,2} & d_{n-2,3} & \dots & d_{n-2,j} & \dots & 1 & 0 & 0 \\ d_{n-1,1} & d_{n-1,2} & d_{n-1,3} & \dots & d_{n-1,j} & \dots & 0 & 1 & 0 \\ d_{n,1} & d_{n,2} & d_{n,3} & \dots & d_{n,j} & \dots & 0 & 0 & 1 \end{bmatrix} \quad (5)$$

- Inverting $[I+D]$ matrix to obtain the correction matrix C .

2.1.5. Double correction. In order to improve the correction of the signal, a double correction was tested. A first correction matrix $C1$ based on the 9 lasers is created as described in the subsection 2.1.4. This correction matrix $C1$ is applied to correct the signal from the 9 lasers used to create it. The corrected signal from the 9 lasers is then used to generate a second correction matrix $C2$. The final signal from a source can be obtained by multiplying the original signal by the matrix product $C1C2$.

2.2. Signal measurement procedure

A small signal, depending on the integration time, is generated by the CCD array detector even when no radiation falls on the CCD element. This dark current increases with the integration time and depends of the characteristics of each pixel [18][28]. Therefore, whenever possible, integration time was chosen to be shorter than 1s [28]. Then, after the reading of raw data Sig_i (counts), the dark current dc_i measured with the same integration time is subtracted. The measured signal $y_{meas,i}$ expressed in counts.s⁻¹ is determined by normalizing it by the integration time. To enhance the dynamic range, measurements are carried out in two stages. The first measurements are done with a suitable integration time $t1$ to acquire the spectrum in the region of its peak value. Second measurements are done to acquire the spectrum outside this region and a higher integration time $t2$ is used to improve signal-to-noise. During the second measurement the instrument then saturates in the region of its peak value, but this region is disregarded and replaced with the data from the first measurement to obtain the final spectrum; this technique is called bracketing. Applying this technique is particularly important when the correction matrix is generated, because the signal-to-noise ratio is relatively weak outside the peak region. Figure 2 illustrates the efficiency of the bracketing technique whereby the signal is more smooth and lower compared to the original signal. This technique has also been used during measurements of actual sources and during calibration.

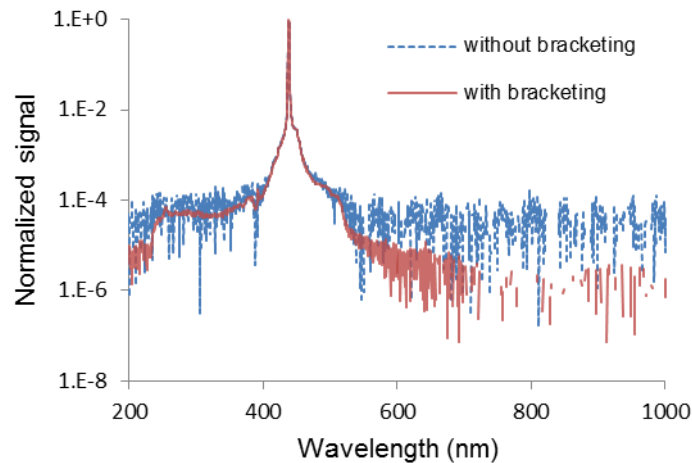


Figure 2. Signal from a laser measured with and without bracketing technique.

2.3. Filters

As mentioned by Zong *et al.* [15], equation 4 does not take into account the stray light δ_{sl} arising from signals outside the spectral range of the spectroradiometer. The level of δ_{sl} depends on the measurable range of the instrument compared to the spectral band response of the CCD. Zong *et al.* [15] proposed to block this out-of-range stray light by filtering these radiation that is using a shortpass filter. Up to now, shortpass filters transmitting radiation at wavelengths within 200 - 1100 nm and rejecting radiation at wavelengths longer than 1100 nm are not available. Except for interferential filters, spectral characteristics of filters are rarely available for wavelengths

shorter than 250nm. Thus effects of δ_{sl} on the signal measured in the UV spectral range was studied using a longpass filter with a cut-on wavelength $\lambda_c=1100nm$ as a shutter. Consequently the measured signal $SigF1100$ with the filter $F1100$ includes the dark current plus the stray light δ_{sl} and the signal measured at each pixel or wavelength is given by:

$$y_{meas_i} = (Sig_i - SigF\lambda_c_i)/t \text{ for } \lambda < \lambda_c, \quad y_{meas_i} = (Sig_i - dc_i)/t \text{ for } \lambda > \lambda_c \quad (6)$$

Two other longpass filters $F425$ and $F800$ help identify which spectral ranges induce constant stray light in the UV range.

Note that filters have an optical density of 4, hence they can be used as a shutter only if the highest signal over the range of measurement of $SigF\lambda_c_i$, with the same integration time and in the absence of the longpass filter, would be lower than 10,000 which is the case with UV radiation from a tungsten halogen lamp.

2.4. Experiment

2.4.1. Spectroradiometers. The two AvaSpec (Avantes, Netherlands) CCD array spectroradiometers used for the experiment cover the wavelength range 200-1100 nm. Both have a 300 lines/mm grating, order sorting filters and a 16-bit AD convertor. The input optics consists of a cosine corrected diffuser coupled to the spectroradiometers using optical fibre. Other individual technical features are described in table 1. A scanning OL 750 spectroradiometer (Optronics Labs, USA) with an integrating sphere for input optics, a double monochromator, order filters and two detectors: photomultipliers and silicon, was used as reference.

Table 1. Technical features of tested spectroradiometers.

Product	Detector	Integration time	FWHM
2048x14	Back-thinned CCD array, 2048x14 pixels	2.2 ms – 10 min	2.4 nm
2048TEC	CCD linear array, 2048 pixels	1.1 ms – 10 min	4.3 nm

2.4.2. Spectral irradiance calibration. CCD spectroradiometers and OL 750 reference was calibrated using two standard sources of spectral irradiance OL 752-12 (Optronics Labs, USA) and OL 752-10 (Optronics Labs, USA). The 30W deuterium lamp (OL752-12) provided the spectral irradiance within the wavelength range of 200 nm to 400 nm and the 200 W tungsten halogen lamp (OL 752-10) the spectral irradiance within the wavelength range of 250 nm to 1100 nm. Spectral calibration factors ($W.m^{-2}.nm^{-1} / Counts.s^{-1}$) are calculated as the ratio of the spectral irradiance of standard lamps to the signal measured at each wavelength.

2.4.3. *Evaluation of correction efficiency.* Risk assessment in the UV-Visible range according to ELV from the European directive 2006/25/EC [11] requires the calculation of the irradiance E_{UVA} and effective irradiances E_{eff} and E_B defined as follow:

$$E_{eff} = \sum_{\lambda=180nm}^{\lambda=400nm} E_{\lambda} S(\lambda) \Delta\lambda, \quad E_{UVA} = \sum_{\lambda=315nm}^{\lambda=400nm} E_{\lambda} \Delta\lambda, \quad E_B = \sum_{\lambda=300nm}^{\lambda=700nm} E_{\lambda} B(\lambda) \Delta\lambda. \quad (7)$$

where $S(\lambda)$ and $B(\lambda)$ are the spectral weighting function taking into account UV radiation effects on eye and skin and blue light radiation effects on eyes, respectively.

Several lamps with various features were measured using CCD spectroradiometers and the OL 750 reference; the purpose was, on the one hand, to compare spectral distributions, and on the other hand, values of E_{eff} , E_{UVA} and E_B , resulting from CCD spectroradiometers to the OL 750 reference.

3. Results

3.1. Correction matrix

The effect of separately changing the width of the IB region as described in sub-section 2.1.2. and the interpolation/extrapolation modes used to generate the correction matrix is illustrated in figure 3. Different correction matrixes of the 2048×14 spectroradiometer were applied to a hypothetical source for which the signal was constant and equal to one at each wavelength.

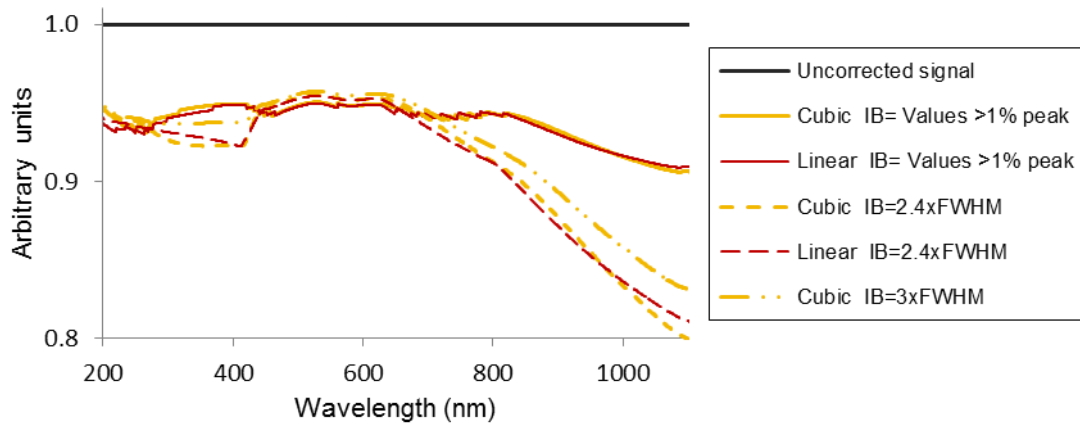


Figure 3. Effect of separately changing the width of the IB region and the interpolation/extrapolation modes used to generate the correction matrix.

As shown in figure 3, there were no significant differences between the cubic interpolation curve (thick solid yellow line) and linear interpolation curve (thin solid red line) when $IB = \text{values} > 1\% \text{ peak}$. Similar results between cubic and linear interpolation methods were obtained when $IB = 2.4 \times FWHM$. Conversely, the levels of corrected signals with the three configurations of IB widths are significantly different within the near infrared region. As the FWHM is wider in the near infrared region than in other spectral ranges the level of the corrected signal decreases when the value fixed for IB decreases. This simulation with a constant spectrum in

particular highlights the correction matrix effects near to the peak region. Due to the lack of constant bandwidth across the spectral range, the adaptive method with $IB = \text{values} > 1\% \text{ peak}$ theoretically gives better results than the fixed IB values.

3.2. Calibration factors

3.2.1. *Experiments with longpass filters.* Before applying the stray light correction, both 2048x14 and 2048 TEC calibrations were normally carried out for both deuterium and tungsten standard lamps as described at §2.4.2 and also by using longpass filters *F1100*, *F800* and *F425* for the tungsten standard lamp as in (6). As the deuterium lamp emits no radiation in the visible and near IR region, the experiment with filters was only applied to the tungsten standard lamp. Matching calibration curves were plotted on figure 4 between 250 and 400 nm where the spectra of the deuterium and tungsten lamps overlap. The calibration curves without stray light correction from the tungsten lamp fall clearly below that of the deuterium lamp (thick solid lines). Both 2048x14 and 2048 TEC calibration curves using *F1100* filter (dotted-dashed line) and those without filter (thick solid lines) are alike, confirming that out-of-range stray light δ_{sl} for wavelengths greater than 1100 nm is negligible. 2048TEC's behaviour is nearly the same with *F800*. On the other hand, the 2048x14 calibration curve with *F800* is slightly higher than the curve without filter proving that a part of the stray light in the UV range arises from near IR. Dotted curves matching both instrument's calibration with *F425* for the tungsten lamp are very close to the calibration curves for the deuterium lamp; thus the stray light on the measured signal in the UV spectral range mainly originates from visible spectral range.

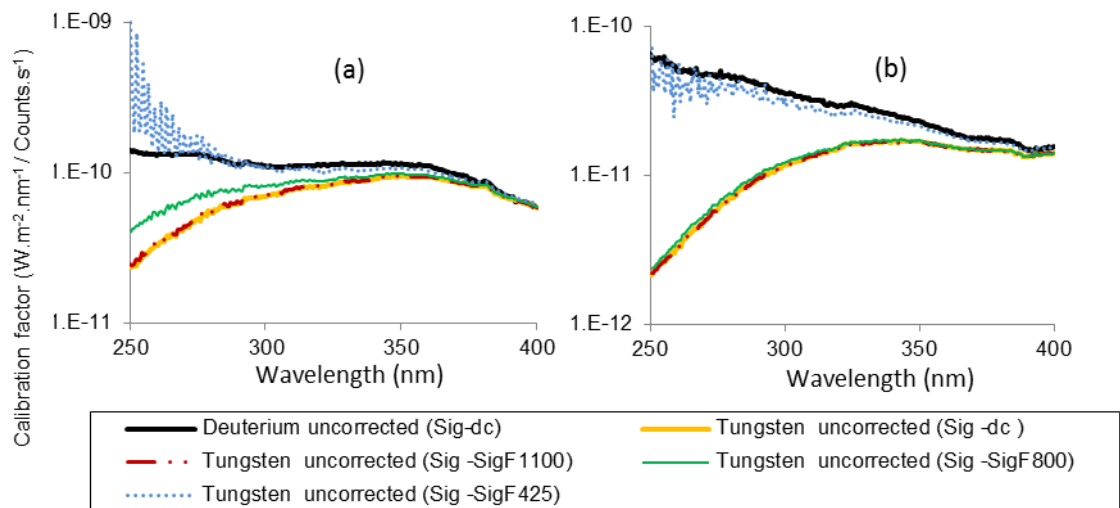


Figure 4. 2048x14 (a) and 2048TEC (b) calibration factors obtained for deuterium and tungsten standard lamps without stray light correction but using longpass filters with the tungsten standard lamp as in (6).

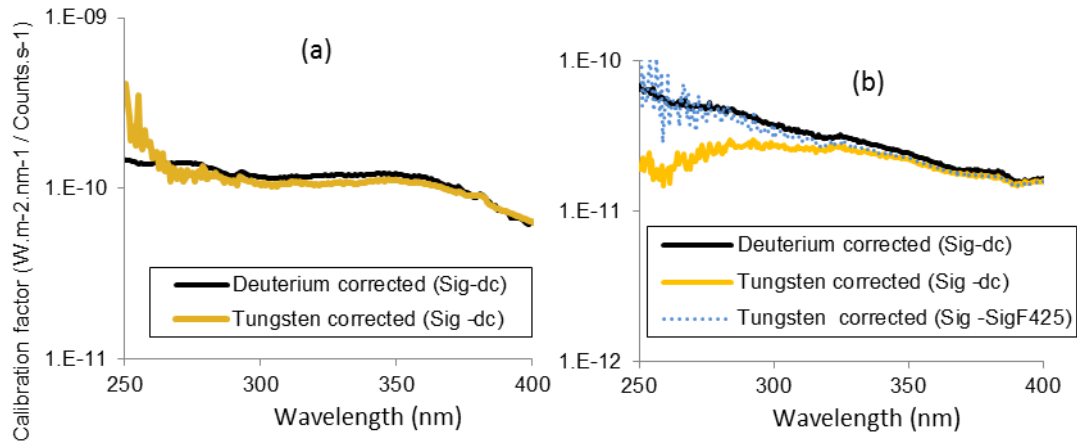


Figure 5. Stray light corrected calibration curves from both 2048x14 (a) and 2048TEC (b) for deuterium and tungsten standard lamps.

3.2.2. *Stray light corrected calibration factors.* Both 2048x14 and 2048 TEC calibrations were carried out for each one of the standard lamps as described in sub-section 2.4.2. The signal from the instruments had been stray light corrected beforehand by using the correction matrix as in equation (4). Like figure 4, figure 5 illustrates these stray light corrected calibration curves from 250 to 400 nm.

The close match of the two curves in figure 5a highlights the fact that the correction matrix enhances the 2048x14 signal from the tungsten lamp between 260 to 400 nm. Nevertheless, the poor signal (weak signal-to-noise ratio) from the tungsten lamp below 260 nm affects the corrected calibration factors.

As the level of stray light from 2048TEC is higher than that of 2048x14 (see tungsten uncorrected ‘sig-dc’ in figure 4), the correction matrix can reduce only a part of the 2048TEC’s stray light. Consequently the best results (dotted line) for this instrument were obtained by a combination of the correction matrix C that removes the stray light component near to the peaks and the $F425$ filter by subtracting the constant component of the stray light arising from visible range. Comparing figure 4b and figure 5b the improvement offered by the combination *correction matrix-F425* against the single $F425$ is about 11% within the wavelength range 250-350 nm. Note that in this configuration, the matrix is only calculated and applied between 200 and 400 nm.

The concatenation of the deuterium curve and the tungsten curve provides the final calibration curve of the spectroradiometers from 200 to 1100 nm used in the study follow-up. To reduce the stray light error the deuterium curve was used from 200 to 380 nm and tungsten lamp beyond 380 nm.

3.3. Spectral distribution

Figure 6 shows examples of comparison of the OL 750 (reference spectroradiometer) and both 2048x14 and 2048TEC spectra for a halogen spotlight and a LED. Each spectral irradiance curve was normalized by its peak value for convenience.

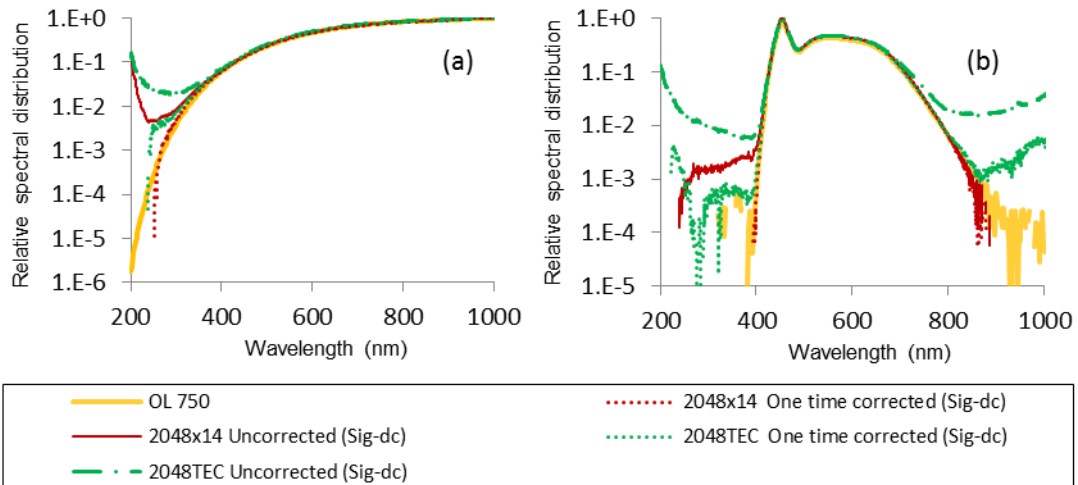


Figure 6. Corrected and uncorrected spectra from a 1500 W halogen spotlight without the protective glass (a) and a LED (b).

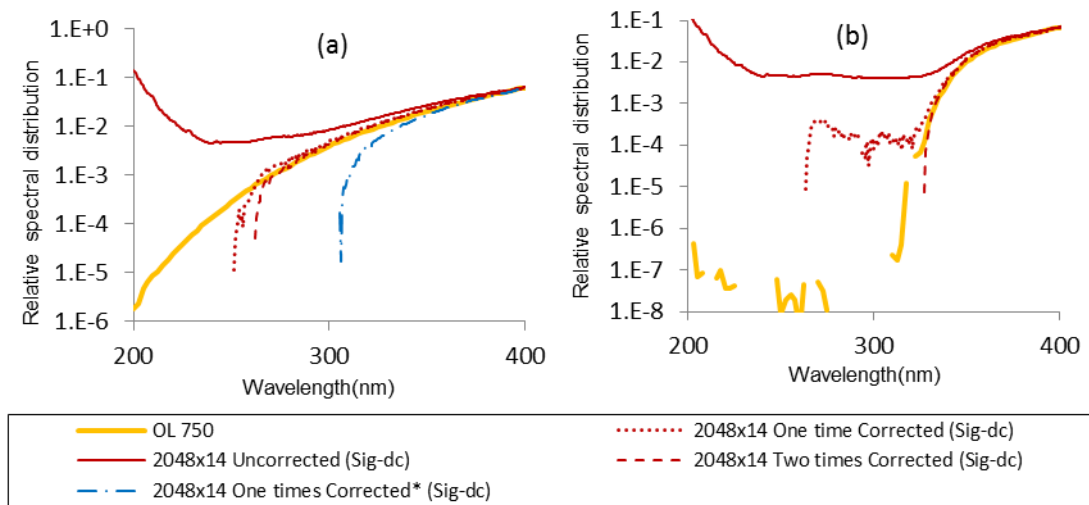


Figure 7. Corrected and uncorrected spectra from a 1500 W halogen spotlight without (a) and with (b) the protective glass.

* One time corrected (Sig-dc) based on a correction matrix generated without bracketing.

As well as results observed during the calibration, the stray light level from 2048TEC is higher than that of 2048x14. There is also stray light for the 2048TEC in the near IR region where a LED is measured (figure 6b). Applying the correction matrix reduces the stray light from the 2048x14 below the minimum detectable level where both spotlights without the protective glass (figure 6a and 7a) and LED (figure 6b) were measured and can reduce that of 2048TEC by 1 or 2 orders of magnitude in the UV and IR regions.

In figure 7b one time correction of the signal from 2048x14 is insufficient to suppress the stray light within the 270-320 nm region where the spotlight is measured with the protective glass. Nevertheless, applying a two time correction matrix provides a spectrum that follows OL 750 closely. Note that one count level of a 16 bit spectroradiometer corresponds to a signal level of 1.5×10^{-5} which accounts for the minimal sensitivity of these spectroradiometers. However, the dynamic range is improved by using bracketing; the impact of bracketing on the results is developed in the sub-section 3.5.

3.4. Risk assessment

Quantities E_{eff} , E_{UVA} and E_B were calculated in compliance with equations 7 on the base of both 2048x14 and 2048TEC corrected and uncorrected spectra. Test lamps were chosen according to their spectra features. The LED, the spotlight and the infrared lamp have continuous spectra while the xenon and the mercury lamps have line spectra. The LED emits only in the visible region, the halogen spotlight emits in all regions and the peak of the emission lies in the near infrared region. Adding a protective glass in front of the spotlight largely reduces the UV radiation below 300 nm. The mercury lamp yields lines in the UV region and the xenon lamp both in the UV and the visible regions. Comparison of results from 2048x14 or 2048TEC with OL 750, are given in tables 2 and 3, respectively.

Table 2. Comparison of E_{eff} , E_{UVA} and E_B calculated on the basis of 2048x14 corrected and uncorrected spectra against OL 750.

Source	Quantities	OL 750	2048x14		
		Values ($W\ m^{-2}$)	Differences between 2048x14 and OL 750 (%)		
			Uncorrected	Corrected 1x	Corrected 2x
LED	E_{eff}	$< 10^{-4}$ ^a	4800	0	0
	E_{UVA}	$< 3.5 \times 10^{-2}$ ^a	0	0	0
	E_B	1.92	-4	-3	-3
Spotlight without protective glass	E_{eff}	2.1×10^{-2}	424	14 (-99) ^b	-10
	E_{UVA}	0.89	11	0 (-17) ^b	-1
	E_B	3.38	-4	-5 (-6) ^b	-5
Spotlight with protective glass	E_{eff}	$< 10^{-4}$ ^a	75900	1700 (2300) ^c	0
	E_{UVA}	0.56	16	0	-2
	E_B	2.98	-4	-4	-4
Infrared lamp	E_{eff}	$< 10^{-4}$ ^a	2570	0	0
	E_{UVA}	$< 3.5 \times 10^{-2}$ ^a	0	0	0
	E_B	1.9×10^{-3}	62	-24	-24
Xenon lamp	E_{eff}	0.32	16	9	9
	E_{UVA}	1.40	4	3	3
	E_B	1.60	-5	-4	-4
Mercury spectral lamp	E_{eff}	5.5×10^{-2}	0	-4	-4
	E_{UVA}	0.12	-6	-9	-8
	E_B	8.1×10^{-2}	-8	-6	-6

^a EN14255-1 [29] and EN 14255-2 [30] standards relating to the measurement and assessment of personal exposure to incoherent radiation in the workplace, require minimal instrument sensitivity set at 1/10 of the applied ELV. As the ELV is expressed in terms of exposure, this minimal value is the ratio of the ELV to the maximal exposure duration. Thus $E_{eff\ min}=10^{-4}\ W.m^{-2}$, $E_{UVA\ min}=3.5 \times 10^{-2}\ W.m^{-2}$ and $E_{B\ min}=10^{-3}\ W.m^{-2}$.

^b Corrected spectrum on the basis of a correction matrix generated without bracketing

^c Source measurement without bracketing

As shown in table 2, the percentage difference between the uncorrected 2048x14 and the OL 750 E_{eff} varies from 0 to 75900%; results from the uncorrected 2048TEC E_{eff} being in the same order (table 3). Significant differences occur when the low level spectral component of broadband sources as LED, spotlight or infrared lamps are measured, confirming what has been recorded in another works [20]. The infrared lamp that emits only in the near IR waveband generates the same effects on the uncorrected 2048x14 E_b (62%); since CCD sensitivity is better in the visible range than in UV, the level of stray light is lower. On the other hand, the percentage difference between the uncorrected 2048x14 and OL 750 E_{eff} , E_{UVA} and E_b from xenon and mercury lamps falls below 16%.

Table 3. Comparison of E_{eff} , E_{UVA} and E_B calculated on the basis of 2048TEC corrected and uncorrected spectra with OL 750.

Source	Quantities	OL 750	2048TEC			
		Values (W m ⁻²)	Differences between 2048TEC and OL 750 (%)			
			Uncorrected	Corrected 1x	Corrected 2x	Corrected 1x (Sig-F425)
LED	E_{eff}	$< 10^{-4}$	45900	1400	690	
	E_{UVA}	$< 3.5 \cdot 10^{-2}$	14	0	0	
	E_B	1.92	-5	-3	-3	
Spotlight without protective glass	E_{eff}	$2.2 \cdot 10^{-2}$	1627	200	150	50
	E_{UVA}	0.93	29	5	3	2
	E_B	3.50	-3	-4	-4	

Applying the correction matrix once on the 2048x14 is sufficient to reduce the percentage difference compared to OL 750 to a level within 0 to 24% for all tested lamps, except the spotlight with the protective glass. However, for this spotlight the difference can be set to 0 by using a two-time correction. Table 3 shows that even a two-time correction of the signal from 2048TEC is insufficient to obtain results close to that of the OL750. Nevertheless, a combination of applying the one-time correction matrix and using a filter *F425* for the spotlight measurement reduces the difference from 1627 % to 50%.

3.5. The effect of bracketing

As describe in sub-section 2.2, the bracketing technique was used during the measurements of laser's signal to generate the correction matrix. To assess the bracketing impact on the results, the spectrum of the spotlight without the protective glass calculated with a correction matrix generated without bracketing is illustrated at figure 7a. The observed effect is an excessive correction of the stray light which leads to suppress any signal below 300 nm. Consequently the risk in the UV region is largely underestimated: the percentage difference in E_{eff} between the 2048x14 and the OL 750 is $\sim -100\%$ (table 2). Note that the same measurements carried out with the spotlight with protective glass gives $E_{eff} < 10^{-4} \text{W.m}^{-2}$ as the OL 750 and in this case the excessive correction cannot be identified. This experiment also shows that a comparison between the corrected spectrum and the reference spectrum is essential to clearly identify an excessive correction and correctly evaluate the efficiency of a numerical correction of the stray light. The effect of the bracketing technique used during the measurement of the sources has also been studied. As shown in table 2, a measurement of the spotlight with the protective glass performed without bracketing produces a noisy signal in the UV region which results in an increase of the percentage difference in E_{eff} .

4. Discussion

As mentioned by Zong *et al.*[15], the stray light correction matrix is largely independent of the bandwidth of the monochromatic radiation because the LSF is normalized by the sum of the

signals within IB band. For this reason, simple lasers instead of tunable lasers could be used in this study. Similar to results recorded by NIST [15] and PTB [22–24] based on about 80 laser lines, experiments carried out in this study show that it is possible to reduce the spectral stray light by one or two orders magnitude by using only nine simple lasers. Because the corrected spectrum has not been compared with a reference spectrum in studies [15, 22–24] and also because the results are dependent of the model of spectroradiometers, as shown in this study, it is not possible to assess the impact of reducing the number of lasers from 80 to 9 on the measurement uncertainty. The method limitations can be tested by further reducing the number of lasers but the selection of the suitable wavelengths of the remaining lasers requires many configurations to be tested, which is time-consuming. For this reason, a single experiment was carried out using only three lasers (266, 589 and 980 nm) to generate the correction matrix. When applying this correction matrix to measurements of the spotlight without the protective glass, a shift of the beginning of the spectrum from 250 nm to 300 nm occurs, showing an excessive correction in the UV range. The percentage difference in E_{eff} between the 2048x14 and the OL 750 is -88%.

Based on a single laser, the correction method developed by Ylianttila [18] appears more simple and cheaper. It provides an adequate accuracy for sunbed UV radiation [18] measurements and for clinical ultraviolet dosimetry [21]. Nevertheless these specific applications need the spectrum for wavelengths above 280 nm to be obtained instead of 200 nm, as required by the European directive 2006/25/EC [11]. Therefore this method might not be efficient for wavelengths below 280 nm. Furthermore extending the algorithm of Ylianttila [18] beyond 400 nm assumes that CCD array spectroradiometers have a constant bandwidth across the spectral range. However, this is not the case. In figure 3, the simulation with a constant spectrum shows that the levels of the corrected signals with $IB=2.4 \times FWHM$ and $IB=value > 1\%$ are significantly different within the near infrared region; the percentage difference between the two corrected signals at 980 nm is about 10%. Even if the UV region suffers from stray light more than other regions, results of the infrared lamp without correction (table2) show that E_b is also affected by the stray light with a measurement uncertainty of 62% compared to the OL 750.

Although this experiment shows that same results are obtained by using only nine simple lasers instead of tunable lasers, a key question is whether this stray light decrease is sufficient when spectroradiometers are intended to assess risk in the workplace. EN14255-1 [29] and EN 14255-2 [30] standards specify that uncertainty shall not exceed 30% for measurements where the results are to be compared with exposure limit values. Corrected quantities E_{UVA} and E_B satisfy this condition; percentage difference between both corrected spectroradiometers (2048x14 and 2048TEC) and the OL 750 do not exceed 24%. Mixed results are obtained regarding E_{eff} , depending on the instrument; 2048x14 provides better results than 2048TEC. Low level of residual stray light in the wavelength band from 220 to 300 nm or in the wavelength calibration [12] results in large errors in the quantification of E_{eff} due to the spectral weighting function $S(\lambda)$, being greatest in this region. Moreover, the required minimal instrument sensitivity to assess E_{eff} is lower by one or two orders of magnitude compared to E_B and E_{UVA} , respectively,

while CCD detectors have lower spectral sensitivity in the UV band than in the visible range. Consequently, the E_{eff} measurement involves using an enhanced detector in the UV band such as the back-thinned CCD array of the 2048x14 instrument for example. If the matrix correction is not sufficient, a combination of correction matrix and a filter can be applied to enhance the results.

The largest stray light errors were observed during measurements of the spotlight with a protective glass for reasons previously described. Thus it is highly inadvisable to assess efficiency of protective goggles in the workplace by measuring radiation from a source through the goggles. It is better, whenever possible, to separately measure radiation emitted from the source in the workplace and transmittance of goggles in the laboratory. Similarly, measurements in the workplace should be intended to assess the risk of industrial processes or specific lamps integrated in industrial processes which cannot be moved. In the case of lamps, measuring the spectrum in laboratory with a double monochromator spectroradiometer would be preferable and give more accurate results.

Since the operational wavelength range (200-1100 nm) of the spectroradiometers used matches the spectral range of the silicon array detector, the stray light δ_{sl} from signals at wavelengths greater than 1100 nm is negligible. Conversely, when the instrument's measurable range is limited to the UV and Visible bands, δ_{sl} is significant, as demonstrated in figure 4a. In this case, a longpass filter which cuts out the signal at 800 nm such as the *F800* filter can replace the shutter. To ensure the measured signal with the filter only comes from the stray light and the dark current, the transmittance of the filter must be below 10^{-5} for a 16 bit AD convertor.

In this study, the assessment of blue-light risk [11] was based on irradiance E_B for convenience, while most situations require radiance L_B to be calculated instead of irradiance E_B . As luminance L of a source is easily measured, L_B can be obtained as follow:

$$L_B = \frac{E_B}{\lambda=780nm} \frac{L}{K \sum_{\lambda=380nm} E_{\lambda} V(\lambda) \Delta\lambda}$$

where $K=683 \text{ lm.W}^{-1}$ and $V(\lambda)$ is the spectral luminous efficiency.

Workplace risk assessment has to cover the whole range 200-3000 nm. In order to complete the spectral range of the CCD spectroradiometers (200-1100 nm), array spectroradiometers covering the region from 900 to 2500 nm can be used. A few measurements with an IR array spectroradiometer have shown that the stray light error is not significant and does not affect spectral measurements to be compared with the ELV.

5. Conclusion

It is important that people in charge of risk assessment of optical radiation in the workplace are aware that using array spectroradiometers can dramatically overestimate the risk when the stray

light error is not corrected. A spectral stray light correction method developed by Zong *et al.* [15] at NIST reduces the stray light error by one or two orders of magnitude and has advantages to be applied in real time. The current study, based on the NIST method, has shown that the same results were obtained by using only nine simple lasers to build the correction matrix, making this method cheaper and more easily implemented by most laboratories.

Regarding the risk assessment in the workplace, this spectral stray light correction method helps determine the exposure level with an acceptable uncertainty for the majority of workplace situations. In some cases, applying a double correction enhances the results. In spite of the efficiency of the matrix correction, E_{eff} quantity may remain affected by a residual stray light error particularly where the UV signal is close to zero or weak compared to the signal in the visible range. The level of uncertainty depends upon the model of spectroradiometers used; the best results are obtained with CCD detectors having an enhanced spectral sensitivity in the UV range. Thus corrected spectroradiometers require a validation against a scanning double monochromator spectroradiometer before using them for risk assessment in the workplace.

To have access to a suitable instrument for risk assessment, further work will consist of implementing a correction matrix and corrected calibration factors in the spectroradiometer's software. Measurements with this instrument will be validated in the workplace.

References

- [1] Murray W E 1990 Ultraviolet radiation exposures in a microbiology laboratory *Health Phys.* **58** 507–10
- [2] Barlier-Salsi A and Salsi S 1998 Lampes à rayonnement ultraviolet - quantification des risques associés à leur utilisation *Cah. Notes Doc.* **170** 49–56
- [3] Salsi S and Barlier-Salsi A 2013 Exposition aux dispositifs d'éclairage scénique : risque pour la santé des professionnels du spectacle vivant ou enregistré *Radioprotection* **48** 391–410
- [4] Martinsons C 2013 Les diodes électroluminescentes et le risque rétinien dû à la lumière bleue *Photoniques* **63** 44–9
- [5] ANSES 2010 *Effets sanitaires des systèmes d'éclairage utilisant des diodes électroluminescentes (LED)* (ANSES)
- [6] Whillock M J, Bandle A M, Todd C D and Driscoll C M H 1990 Measurements and hazard assessment of the optical emissions from various industrial infrared sources *J. Radiol. Prot.* **10** 43–6
- [7] Barlier A 1994 Rayonnements optiques dans une forge - mesures et moyens de protection *Cah. Notes Doc.* **155** 181–93
- [8] ICNIRP 2004 Guidelines on limits of exposure to ultraviolet radiation of wavelengths 180 nm to 400 nm (incoherent optical radiation) *Health Phys.* **87** 171–86
- [9] ICNIRP 1997 Guidelines on limits of exposure to broad-band incoherent optical radiation (0.38 to 3 μm) *Health Phys.* **73** 539–54
- [10] ICNIRP 2013 ICNIRP guidelines on limits exposure to incoherent visible and infrared radiation *Health Phys.* **105** 74–91
- [11] European Union 2006 Directive 2006/25/EC of the european parliament and of the council of 5 April 2006 on minimum health and safety requirements regarding the exposure of workers to risks arising from physical agents (artificial optical radiation) *Off. J. Eur. Union* **L114** 38 – 59

- [12] Trevelyan F 2011 The use of clinical broadband UV radiometers for optical radiation hazard measurement *J. Radiol. Prot.* **31** 453–65
- [13] Reed N G, Wengrattis S and Sliney D H 2009 Intercomparison of instruments used for safety and performance measurements of ultraviolet germicidal irradiation lamps *J. Occup. Environmental Hyg.* **6** 289–97
- [14] Barlier-Salsi A and Salsi S 2010 Mesures des rayonnements optiques aux postes de travail : comparaison de différentes méthodes et matériels de mesure *Radioprotection* **45** 307–20
- [15] Zong Y, Brown S W, Johnson B C, Lyckke K R and Ohno Y 2006 Simple spectral stray light correction method for array spectroradiometer *Appl. Opt.* **45** 1111–9
- [16] Shaw M and Goodman T 2008 Array-based goniospectroradiometer for measurement of spectral radiant intensity and spectral total of light sources *Appl. Opt.* **47** 2637–47
- [17] Shen H S, Pan J, Feng H and Liu M 2009 Stray light errors in spectral colour measurement and two rejection methods *Metrologia* **46** 129–35
- [18] Ylianttila L, Visuri R, Huurto L and Jokela K 2005 Evaluation of a single-monochromator diode array spectroradiometer for sunbed UV-radiation measurements *Photochem. Photobiol.* **81** 333–41
- [19] Brown S W, Johnson B C, Feinholz M E, Yarbrough M A, Flora S J, Lyckke K R and Clark D K 2003 Stray light correction algorithm for spectrographs *Metrologia* **40** 81–4
- [20] Zong Y, Brown S W, Lykke K R and Ohno Y 2007 Correction of straylight in spectroradiometers and imaging instruments *Proceedings of 26 CIE th session (BEIJING)*
- [21] Coleman A, Sarkany R and Walker S 2008 Clinical ultraviolet dosimetry with a CCD monochromator array spectroradiometer *Phys. Med. Biol.* **53** 5239–55
- [22] Sperling A, Larionov O, Grusemann U and Winter S 2005 Stray-light correction of array spectrometers using tuneable pulsed and cw lasers *Proceedings of the 9th international conference on new developments and applications in optical radiometry (NEWRAD)* Davos p 93
- [23] Sperling A 2011 Tuneable lasers at PTB for photometry and radiometry *NewRAD 2011 Abstract collection NEWRAD conference (Maui (Hawaii))* pp 10–11
- [24] Nevas S, Sperling A and Oderkerk B 2012 Transferability of stray light corrections among array spectroradiometers *AIP conference proceedings 1531,821(2013)* AIP conference (Berlin)
- [25] Kreuter A and Blumthaler M 2009 Stray light correction for solar measurements using array spectrometers *Review Sci. Instrum.* **80** 1–3
- [26] Salim S G R, Fox N G P, Hartree W S, Woolliams E R, Sun T and Grattan K T V 2011 Stray light correction for diode-array-based spectrometers using a monochromator *Appl. Opt.* **50** 5130–8
- [27] Feinholz M E, Flora S J, Brown S W, Zong Y, Lykke K R, Yarbrough M A, Johnson B C and Clark D K 2012 Stray light correction algorithm for multichannel hyperspectral spectrographs *Appl. Opt.* **51** 3631–41
- [28] Zonios G 2010 Noise and stray light characterization of a compact CCD spectrophotometer used in biomedical applications *Appl. Opt.* **49** 163–9
- [29] EN 14255-1 2005 Measurement and assessment of personal exposures to incoherent optical radiation - part 1: Ultraviolet radiation emitted by artificial sources in the workplace *AFNOR* 29
- [30] EN 14255-2 2006 Measurement and assessment of personal exposures to incoherent optical radiation - part 2: Visible and infrared radiation emitted by artificial sources in the workplace *AFNOR* 43